Chemical Engineering Science 65 (2010) 1705–1719

Contents lists available at ScienceDirect

Chemical Engineering Science

journal homepage: www.elsevier.com/locate/ces

An ideal point method for the design of compromise experiments to simultaneously estimate the parameters of rival mathematical models

Brecht M.R. Donckels [a,b], Dirk J.W. De Pauw [b], Peter A. Vanrolleghem [c], Bernard De Baets [b,*]

[a] BIOMATH, Department of Applied Mathematics, Biometrics and Process Control, Ghent University, Coupure links 653, B-9000 Ghent, Belgium
[b] KERMIT, Department of Applied Mathematics, Biometrics and Process Control, Ghent University, Coupure links 653, B-9000 Ghent, Belgium
[c] modelEAU, Département de génie civil, Pavillon Pouliot, Université Laval, Québec, QC, Canada G1K 7P4

ARTICLE INFO

Article history:
Received 24 November 2008
Received in revised form
9 November 2009
Accepted 11 November 2009
Available online 22 December 2009

Keywords:
Mathematical modelling
Optimal experimental design
Model discrimination
Parameter estimation
Kinetics
Dynamic simulation
(Bio)chemical engineering

ABSTRACT

When several rival mathematical models are proposed for one and the same process, experimental design techniques are available to design optimal discriminatory experiments. Because these techniques are model-based, it is important that the model predictions are not too uncertain. Therefore, model discrimination may become more efficient and effective if this uncertainty is reduced first. This can be achieved by performing experiments designed to increase the accuracy of the parameter estimates and, thus, the model predictions. However, performing such an additional experiment for each rival model may undermine the overall goal of optimal experimental design, which is to minimize the experimental effort. This paper deals with the design of a so-called compromise experiment, which is an experiment that is not optimal for each of the rival models, but sufficiently informative to improve the overall accuracy of the parameters of all rival models. For this purpose, the problem is approached as a multi-objective optimization problem and the ideal point method is proposed to design the compromise experiment. This method searches for the experiment that is as close as possible to the optimal experiments of the individual rival models. The method is applied to a case study where nine rival models are competing to describe the kinetics of an enzymatic reaction, and the obtained results show that the ideal method is capable of designing a compromise experiment.

1. Introduction

Mathematical models are increasingly used for the design, optimization and control of sometimes complex processes (e.g., in Dochain and Vanrolleghem, 2001; Hoffmann et al., 2002; Jiang et al., 2005; Kitano, 2002; Lee et al., 1999). However, when insight in a process is insufficient, several hypotheses can be postulated on how the process actually works. Each of these hypotheses can subsequently be translated into a unique model structure, and a set of rival models for the process arises.

Obviously, one is especially interested in the model that describes the process under study in the most appropriate way. To identify this model from a set of rival models, it may be necessary to collect new information about the process, and thus additional experiments have to be performed. Because the latter is usually time- and money-consuming, carefully designing these experiments can significantly reduce the required experimental effort. To achieve model discrimination in a minimal number of experiments, experimental design methods described in literature can be used (Buzzi-Ferraris et al., 1984; Chen and Asprey, 2003; Donckels et al., 2009a; Hunter and Reiner, 1965; Vanrolleghem and Van Daele, 1994).

Common to the experimental design methods is the fact that they are model-based, which means that potential experiments are judged *in silico* based on how the rival models predict their outcome. In this respect, the importance of the uncertainty on the model predictions cannot be overstated. Indeed, when this uncertainty is too large, the expected differences in the model predictions may not occur after all, which undermines the efficacy and efficiency of the model discrimination procedure (Burke et al., 1996, 1997; Buzzi-Ferraris et al., 1984; Chen and Asprey, 2003; Donckels et al., 2009a; Kremling et al., 2004; Schwaab et al., 2006; Ternbach et al., 2005).

The uncertainty on the model predictions is indirectly determined by the quality of the data that is used to estimate the model parameters. When the data are uninformative with regard to the model parameters, their estimates will be poor and the model predictions will be unreliable. Nevertheless, the classical approach is to deal with the problems of model discrimination and accurate parameter estimation successively (Dochain and Vanrolleghem, 2001; Vanrolleghem and Dochain, 1998; Walter and Pronzato, 1997). First, experiments are designed and performed to choose between the rival model structures, even when the parameter estimates are inaccurate. Then, once the

* Corresponding author.
E-mail address: bernard.debaets@ugent.be (B. De Baets).

0009-2509/$ - see front matter © 2009 Elsevier Ltd. All rights reserved.
doi:10.1016/j.ces.2009.11.009

most promising model structure has been selected, experiments are designed and performed to increase the accuracy of its parameters (for instance, using the methods described in Baltes et al., 1994; Munack, 1991; Vanrolleghem and Dochain, 1998; Walter and Pronzato, 1997).

An interesting variant of this approach has been proposed by Hill et al. (1968), who introduced a joint criterion that focuses on both model discrimination and parameter estimation. They state that an experimental design procedure should emphasize model discrimination when there is substantial uncertainty as to which model is the most appropriate one and emphasize parameter estimation when one of the rival models seems to be overwhelmingly superior to the others. In other words, a balance between the two tasks is sought, which is different from simply following the heuristic: model discrimination first, then precise parameter estimation. Still, as with the classical approach, the model discrimination procedure starts with the design of an optimal discriminatory experiment, while the emphasis gradually shifts to parameter estimation as experimentation progresses and discrimination becomes possible.

The discrimination among several rival models may thus become more effective and efficient if the uncertainty on the parameter estimates, and consequently on the model predictions, can be reduced prior to the start of the model discrimination procedure. This can be achieved by designing and performing experiments dedicated to increase the accuracy of the parameter estimates. However, performing an additional experiment for each rival model may undermine the overall goal of optimal experimental design, since this would require at least as many experiments as the number of rival models. Therefore, a so-called compromise experiment could be designed and performed. Such an experiment is not optimal for one or more of the individual rival models, but is sufficiently informative to improve the overall accuracy of the parameters of all rival models.

The design of a compromise experiment was already studied in Donckels et al. (2009b), where a kernel-based method was presented and demonstrated for experimental design exercises where one is interested in finding the optimal sampling times, and the work of Dette and Kwiecien (2004), Läuter (1974) who introduced the term model-robust designs. In this paper, the idea of designing a compromise experiment is further explored by treating it as a multi-objective problem. The so-called ideal point method proposed in this paper can be used for experimental design problems with experimental degrees of freedom of any type (manipulations, initial conditions and sampling times), where this would be difficult with the kernel-based method described in Donckels et al. (2009b).

The paper is organized as follows. In Section 2, the theory on parameter estimation and optimal experimental design for parameter estimation is explained, as well as the ideal point method to design a compromise experiment. This method is illustrated on a case study in Section 3, where a number of models is proposed to describe the kinetics of an enzyme. The capability of the ideal point method to design a compromise experiment is evaluated and, where possible, compared to that of the kernel-based method previously published in Donckels et al. (2009b). The conclusions drawn from these results are listed in Section 4.

2. Methods

2.1. Mathematical model representation

In what follows, general deterministic models in the form of a set of (possibly mixed) differential and algebraic equations are considered, using the following notations:

$$\dot{\boldsymbol{x}}(t) = \boldsymbol{f}(\boldsymbol{x}(t), \boldsymbol{u}(t), \boldsymbol{\theta}, t), \quad \boldsymbol{x}(t_0) = \boldsymbol{x}_0, \tag{1}$$

$$\hat{\boldsymbol{y}}(t) = \boldsymbol{g}(\boldsymbol{x}(t)), \tag{2}$$

where $\boldsymbol{x}(t)$ is an n_s- dimensional vector of time-dependent state variables, $\boldsymbol{u}(t)$ is an n_u- dimensional vector of time-varying inputs to the process, $\boldsymbol{\theta}$ is an n_p- dimensional vector of model parameters taken from a continuous, realizable set $\boldsymbol{\Theta}$, and $\hat{\boldsymbol{y}}(t)$ is an n_m-dimensional vector of measured response variables that are function of the state variables, $\boldsymbol{x}(t)$. An experiment will be denoted as ξ, and is determined by the values of the experimental degrees of freedom, such as sampling times, initial conditions and time-varying or constant process inputs (manipulations).

2.2. Parameter estimation

The values of the model parameters, which by definition do not change during the course of the simulation, have to be determined from experimental data in a process called parameter estimation. It consists of minimizing the weighted sum of squared errors (WSSE) functional through an optimal choice of the parameters $\boldsymbol{\theta}$. This can be written as

$$\hat{\boldsymbol{\theta}} = \underset{\boldsymbol{\theta} \in \boldsymbol{\Theta}}{\operatorname{argmin}} \mathrm{WSSE}(\boldsymbol{\theta}), \tag{3}$$

where $\mathrm{WSSE}(\boldsymbol{\theta})$ is calculated as

$$\mathrm{WSSE}(\boldsymbol{\theta}) = \sum_{k=1}^{n_e} \sum_{l=1}^{n_{sp_k}} \Delta\hat{\boldsymbol{y}}(\xi_k, \boldsymbol{\theta}, t_l)' \cdot \mathbf{Q} \cdot \Delta\hat{\boldsymbol{y}}(\xi_k, \boldsymbol{\theta}, t_l) \tag{4}$$

and

$$\Delta\hat{\boldsymbol{y}}(\xi_k, \boldsymbol{\theta}, t_l) = \boldsymbol{y}(\xi_k, t_l) - \hat{\boldsymbol{y}}(\xi_k, \boldsymbol{\theta}, t_l) \tag{5}$$

represents the difference between the vector of the n_m measured response variables and the model predictions at time t_l ($l = 1, \ldots, n_{sp_k}$) of experiment ξ_k ($k = 1, \ldots, n_e$). Further, n_e represents the number of experiments from which data are used to estimate the model parameters, n_{sp_k} represents the number of sampling times in experiment ξ_k, which are assumed to be the same for all measured state variables, and $\mathbf{Q}$ is an n_m-dimensional square matrix of user-supplied weighing coefficients. Typically, a Gaussian distribution is assumed for the measurement errors, and $\mathbf{Q}$ is chosen as the inverse of the measurement error covariance matrix $\boldsymbol{\Sigma}$ to incorporate the measurement uncertainty in the WSSE (Marsili-Libelli et al., 2003; Omlin and Reichert, 1999; Vanrolleghem and Dochain, 1998).

2.3. Optimal experimental design for parameter estimation

In this section, the methodology used to design experiments to obtain more accurate parameter estimates, often called optimal experimental design for parameter estimation (OED/PE), is briefly described.

2.3.1. Fisher information matrix

As stated before, the accuracy of the parameter estimates highly depends on the quality or the information content of the experimental data from which they are determined. The information content of n_e experiments, $\xi_1, \ldots, \xi_{n_e}$, with regard to the model parameters is represented by the so-called Fisher information matrix (**FIM**) (Goodwin and Payne, 1977; Ljung, 1999; Mehra, 1974; Munack, 1991; Vanrolleghem and Dochain, 1998; Walter and Pronzato, 1997), which is calculated as

$$\mathbf{FIM}(\xi_1, \ldots, \xi_{n_e}, \hat{\boldsymbol{\theta}}) = \sum_{k=1}^{n_e} \mathbf{FIM}(\xi_k, \hat{\boldsymbol{\theta}}), \tag{6}$$

where

$$\mathbf{FIM}(\xi_k,\hat{\boldsymbol{\theta}})=\sum_{l=1}^{n_{sp_k}}\left(\frac{\partial\hat{\mathbf{y}}}{\partial\boldsymbol{\theta}}(\xi_k,\boldsymbol{\theta},t_l)\Big|_{\hat{\boldsymbol{\theta}}}\right)'\cdot\boldsymbol{\Sigma}(\xi_k,t_l)^{-1}\cdot\left(\frac{\partial\hat{\mathbf{y}}}{\partial\boldsymbol{\theta}}(\xi_k,\boldsymbol{\theta},t_l)\Big|_{\hat{\boldsymbol{\theta}}}\right). \quad (7)$$

A closer look at Eq. (7) shows that the **FIM** is composed of two components, the parameter sensitivities ($\partial\hat{\mathbf{y}}/\partial\boldsymbol{\theta}$) and the measurement error covariance matrix ($\boldsymbol{\Sigma}$). The parameter sensitivity with respect to a certain state variable expresses how much that state variable will change when a parameter is slightly perturbed. A state variable that is highly sensitive to a certain parameter will therefore contain a lot of information about this parameter, while a variable that is insensitive to the parameter does not contribute to the information content for that parameter. The role of the measurement error covariance matrix in the calculation of the **FIM** is rather straightforward, since it is obvious that a measurement associated with a large measurement error will contribute less to the information content than a measurement with a small measurement error.

2.3.2. Central rationale behind optimal experimental design for parameter estimation

In general, optimal experimental design is an optimization problem, where the optimum of a well-defined objective function is sought by varying the experimental degrees of freedom. The experimental degrees of freedom, ξ, are restricted by a number of constraints that define a set of possible experiments, denoted as Ξ. These constraints are determined by the experimental setup and are specified before the start of the experimental design exercise.

The Fisher information matrix described in the previous section expresses the information content of the n_e experiments with regard to the model parameters, and its maximization is the central rationale behind optimal experimental design for parameter estimation (Asprey and Macchietto, 2000; Goodwin and Payne, 1977; Ljung, 1999; Mehra, 1974; Munack, 1991; Shirt et al., 1994; Vanrolleghem and Dochain, 1998; Walter and Pronzato, 1997). The (n_e+1) th experiment, denoted as $\xi^{\star}_{n_e+1}$, is obtained as

$$\xi^{\star}_{n_e+1}=\underset{\xi\in\Xi}{\operatorname{argmax}}\,\gamma(\mathbf{FIM}(\xi_1,\ldots,\xi_{n_e+1},\hat{\boldsymbol{\theta}}_{n_e})), \quad (8)$$

with

$$\mathbf{FIM}(\xi_1,\ldots,\xi_{n_e+1},\hat{\boldsymbol{\theta}}_{n_e})=\sum_{k=1}^{n_e}\mathbf{FIM}(\xi_k,\hat{\boldsymbol{\theta}}_{n_e})+\mathbf{FIM}(\xi_{n_e+1},\hat{\boldsymbol{\theta}}_{n_e}). \quad (9)$$

The information content of the proposed (n_e+1) th experiment, which is represented by a scalar function (γ) of the $\mathbf{FIM}(\xi_{n_e+1},\hat{\boldsymbol{\theta}}_{n_e})$, is thus maximized (see Section 2.3.3), given the information content of the already performed experiments ($\mathbf{FIM}(\xi_1,\ldots,\xi_{n_e},\hat{\boldsymbol{\theta}}_{n_e})$) and the parameter values derived from these experiments ($\hat{\boldsymbol{\theta}}_{n_e}$). For simplicity, $\mathbf{FIM}(\xi_1,\ldots,\xi_{n_e+1},\hat{\boldsymbol{\theta}}_{n_e})$ will be denoted as **FIM** in the following.

2.3.3. Experimental design criteria based on the *FIM*

Since the **FIM** is a matrix, it cannot be maximized as such. Therefore, several design criteria/objective functions have been proposed based on the **FIM** (Atkinson and Donev, 1992; Munack, 1991; Petersen, 2000; Vanrolleghem and Dochain, 1998), all of which exploit the inversely proportional relationship between the **FIM** and the parameter estimation error covariance matrix. This relationship is dictated by the Cramér–Rao inequality (Ljung, 1999; Walter and Pronzato, 1997), which states that under certain conditions (that is, uncorrelated white measurement noise), the inverse of the **FIM** gives a lower bound of the parameter estimation error covariance matrix. In this way, properties of the **FIM** determine the size, shape and orientation of the confidence region of the parameter estimates, and thus their accuracy.

In this paper, only the so-called D-optimality design criterion will be discussed and applied. With this criterion, the determinant of the **FIM** is maximized. The latter is inversely proportional to the volume of the confidence region of the parameter estimates, and this volume is thus minimized when maximizing det(**FIM**). In other words, one minimizes the geometric average of the variances of the parameter estimates. In this respect, it is important to be aware of the fact that the value of the D-optimality design criterion scales with the number of model parameters (Atkinson and Donev, 1992; Ljung, 1999; Walter and Pronzato, 1997). Moreover, D-optimal experiments possess the property of being invariant with respect to any rescaling of the parameters (Petersen, 2000; Seber and Wild, 1989).

The effect of this criterion on the confidence region is illustrated in Fig. 1 for an estimation problem with two parameters (θ_1 and θ_2). The size, shape and orientation of the confidence region, which is an ellipse in the case of two parameters, are determined by the eigenvalues and eigenvectors of the **FIM**. The largest axis of the confidence ellipse is inversely proportional to the square root of the smallest eigenvalue (λ_{min}), while the smallest axis is inversely proportional to the square root of the largest eigenvalue (λ_{max}).

2.4. Design of a compromise experiment

This paper investigates the possibility to design a compromise experiment, that is, an experiment which may not be optimal for each individual rival model, but sufficiently informative to improve the overall accuracy of the parameters of all rival models. As stated in the Introduction, this problem was already tackled for the case where only the sampling times are to be optimized (Donckels et al., 2009b). The basic idea of the kernel-based method presented there is briefly discussed in Section 2.4.1, and is illustrated in Fig. 2.

2.4.1. Description of the kernel-based method (Donckels et al., 2009b)

The kernel-based method starts with the determination of the optimal sampling times for the individual models (black and gray dots in Fig. 2). Then, these sampling times are collected on one time axis, and Gaussian-like kernel functions (denoted as κ) are imposed on each sampling time (dashed lines). The sum of these kernel functions (full line), given by

$$\hat{p}(t)=\sum_{i=1}^{m}\sum_{j=1}^{n_{sp}}w_{ij}\cdot\kappa\left(\frac{t-t_{ij}}{h}\right) \quad (10)$$

is used to determine the compromise sampling times (as illustrated in Fig. 2). In Eq. (10), t_{ij} represents the j th sampling

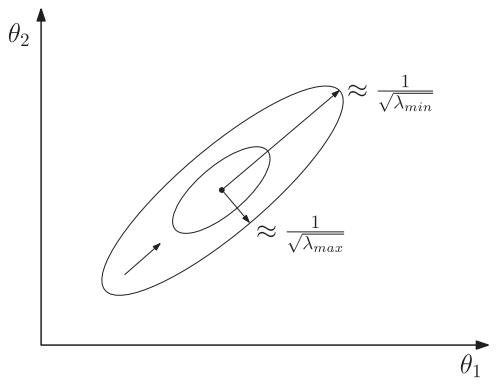

Fig. 1. Illustration of the D-optimality design criterion that causes the volume of the confidence region to decrease.

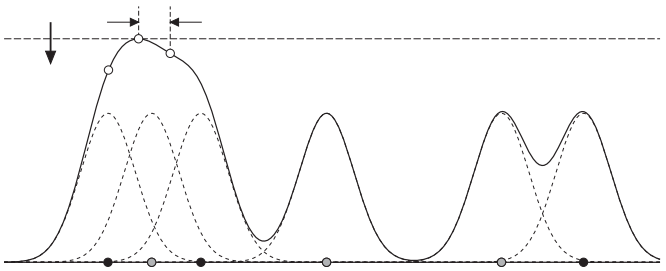

Fig. 2. The black dots represent the optimal sampling times for model i, whereas the gray ones represent those for model j. The compromise sampling times (location is indicated by the white dots) are those that maximize $\hat{p}(t)$ (represented by the full line) under the constraint that a minimum time between two sampling times is required.

time that was found to be optimal for model i, h represents the so-called smoothing parameter, and w_{ij} represents the weight of the j th sampling time of the optimal experiment for model i (t_{ij}). The latter represent the contribution of the individual samples to the information content of the experiment. The kernel function is given by

$$\kappa\left(\frac{t-t_{ij}}{h}\right) = e^{-((t-t_{ij})/h)^2}. \tag{11}$$

The fact that sampling times that are close to each other enforce each other (for instance, for the sampling times on the left in Fig. 2) agrees with the rationale that the compromise sampling times are located in regions that are interesting for several rival models. For more details about this method the reader is referred to Donckels et al. (2009b).

As stated before, this method focusses on finding compromise sampling times, and extending the method for cases where all types of experimental degrees of freedom (manipulations, initial conditions and sampling times) are considered, appears to be rather complicated. For instance, the method requires the choice of a so-called smoothing parameter which determines the width of the kernel functions. For the case where only sampling times were optimized, this smoothing parameter could be linked to and calculated from the required minimum time interval between two measurements, which is dictated by the experimental setup. For other experimental degrees of freedom, such as the initial conditions of certain process variables or the timing of a pulse, such an approach is not straightforward, which makes it difficult to choose this smoothing parameter in an objective manner.

Therefore, an alternative method is presented in this paper, that is able to cope with experimental design problems where experimental degrees of freedom of all types are considered. Since the optimal experiment for model m_i may not be optimal for model m_j, the experimental design problem can be seen as a multi-objective problem, where the aim is to systematically and simultaneously optimize (that is, maximize or minimize) a number of possibly conflicting objectives, each of which is translated into an objective function. Without loss of generality, it is assumed in the following that the aim of the optimization exercise is to minimize these objective functions.

2.4.2. Multi-objective optimization problems

A general multi-objective optimization problem is posed as (Deb, 2001; Marler and Arora, 2004)

$$\min_{\boldsymbol{x}\in\boldsymbol{X}} \boldsymbol{F}(\boldsymbol{x}) \equiv [f_1(\boldsymbol{x}), f_2(\boldsymbol{x}), \ldots, f_d(\boldsymbol{x})]', \tag{12}$$

where $\boldsymbol{x} = [x_1, x_2, \ldots, x_q]' \in \boldsymbol{X}$ represents the q-dimensional design or decision vector, $\boldsymbol{X}$ represents the feasible design or decision space, and $\boldsymbol{F}(\boldsymbol{x})$ represents the d-dimensional vector containing the individual objective function values $f_i(\boldsymbol{x})$. The feasible criterion

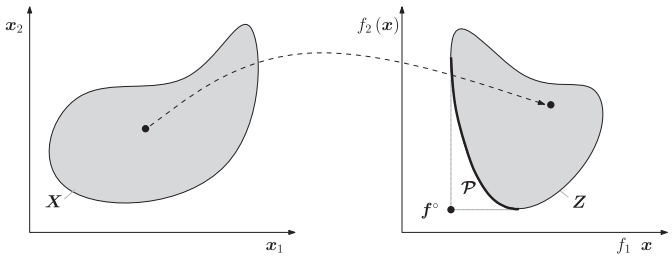

Fig. 3. Feasible design space ($\boldsymbol{X}$) and feasible criterion space ($\boldsymbol{Z}$) for a hypothetical multi-objective problem with two design variables ($\boldsymbol{x}_1$ and $\boldsymbol{x}_2$) where the aim is to simultaneously minimize two objective functions (f_1 and f_2). In addition, the Pareto-optimal front ($\mathcal{P}$) and the ideal point ($\boldsymbol{f}^\circ$) are shown.

space, denoted as $\boldsymbol{Z}$, is defined as the set $\{\boldsymbol{F}(\boldsymbol{x})|\boldsymbol{x}\in\boldsymbol{X}\}$ (Deb, 2001; Marler and Arora, 2004).

In this respect, it is important to realize that each point in the design space maps to a point in the criterion space (see Fig. 3), but the reverse may not be true. For instance, in general, there does not exist a vector $\boldsymbol{x}$ for which each objective function is minimal. The point in criterion space that is formed by the individual minima of the different objective functions is called the ideal point (Deb, 2001), denoted as $\boldsymbol{f}^\circ$ and defined as follows:

$$\boldsymbol{f}^\circ = \left[\min_{\boldsymbol{x}\in\boldsymbol{X}} f_1(\boldsymbol{x}), \min_{\boldsymbol{x}\in\boldsymbol{X}} f_2(\boldsymbol{x}), \ldots, \min_{\boldsymbol{x}\in\boldsymbol{X}} f_d(\boldsymbol{x})\right]'. \tag{13}$$

In an experimental design context, $\boldsymbol{x}$ represents an experiment, denoted as ξ, and $\boldsymbol{X}$ represents the set of all possible experiments, denoted as Ξ. The objective functions correspond to the D-optimality design criteria associated with each of the rival models. So, the number of objective functions equals the number of rival models. Note that also other design criteria, which were not described in this paper, could have been used (e.g., A-optimality, modE-optimality, or even the cost of an experiment). For more information on these design criteria, the reader is referred to Atkinson and Donev (1992), Munack (1991), Petersen (2000), and Vanrolleghem and Dochain (1998).

2.4.3. Solving multi-objective optimization problems

In contrast to single-objective optimization, a solution to a multi-objective problem is more a concept than a definition. In the case of conflicting objective functions, the resulting multi-objective optimization problem gives rise to a set of points that all fit a predetermined definition of an optimum (Deb, 2001). The predominant concept in defining an optimal point is that of Pareto-optimality, which is defined as follows:

Definition 2.1. A point, $\boldsymbol{x}^\star \in \boldsymbol{X}$, is Pareto-optimal if there does not exist another point, $\boldsymbol{x}\in\boldsymbol{X}$, such that $\boldsymbol{f}(\boldsymbol{x}) \leq \boldsymbol{f}(\boldsymbol{x}^\star)$, and $f_i(\boldsymbol{x}) < f_i(\boldsymbol{x}^\star)$ for at least one objective function.

In words, a point is Pareto-optimal if there is no other point that improves at least one objective function without worsening another objective function. The set of all Pareto-optimal is known as the Pareto-front, denoted as $\mathcal{P}$ and shown in Fig. 3. Each point located on this front may thus in a sense be considered as optimal. In practice, one or some of the Pareto-optimal points will eventually be selected by the decision maker.

However, although several optimization algorithms are described in literature to determine the Pareto front (Deb, 2001), it often appears to be a difficult and computationally demanding task (Deb, 2001; Goel et al., 2007). This is especially true for the optimal experimental design applications focussed on in this paper, where the evaluation of an experiment proposed by the optimization algorithm involves several model simulations. In addition, the problem of finding the Pareto front may become

prohibitively complex as the number of objectives increases, and visualizing the Pareto front is difficult for problems with more than three dimensions. The latter is important because the Pareto front will eventually be used as a reference by the decision maker/experimenter, who has to choose which experiment will be performed.

2.4.4. The ideal point method

To overcome the issues raised above, multi-objective problems are often translated into single-objective problems. The latter approach is also proposed in this paper, where the optimal solution is defined as the point that is as close as possible to the ideal point (defined above), and for which all individual objective functions are thus as close as possible to their corresponding minima (Deb, 2001; Marler and Arora, 2004). The presented method is often called the ideal point method (Deb, 2001), and this terminology will be used in the following.

To define closeness, different mathematical measures of distance can be used, such as the ℓ_p distance function (or Minkowski distance function) (Deb, 2001). The ℓ_p distance of any point in criterion space $\boldsymbol{x}$ from the ideal point $\boldsymbol{f}^\circ$ can be calculated as

$$\ell_p(\boldsymbol{x}) = \left(\sum_{i=1}^{d} |f_i(\boldsymbol{x}) - f_i^\circ|^p \right)^{1/p}, \tag{14}$$

where p can take any value between 1 and $+\infty$. In this paper, only the ℓ_1, the ℓ_2 and the ℓ_∞ distance functions are considered.

When the ℓ_1 distance function ($p=1$) is used, the multi-objective problem reduces to a single-objective problem where the different objective functions are simply summed. Note that this ℓ_1 distance function is also known as the taxicab distance or the Manhattan distance. When the ℓ_2 distance function ($p=2$) is used, the Euclidean distance between the ideal point and any point in criterion space is minimized. For larger values of p, the largest term of Eq. (14) will dominate the value of $\ell_p(\boldsymbol{x})$ more and more, and the distance function associated with $p=+\infty$ (also called the Chebyshev distance function) eventually becomes

$$\ell_\infty(\boldsymbol{x}) = \max_{i=1,\ldots,d} |f_i(\boldsymbol{x}) - f_i^\circ|. \tag{15}$$

The multi-objective problem thus reduces to a problem where the maximal deviation from the ideal point is minimized. The working principle of the ideal point method for each of these three distance functions discussed above is shown in Figs. 4, 5 and 6, respectively.

In an experimental design context, the ideal point is defined by the optimal experiments for the individual models. When the D-optimality design criterion is used (which corresponds to $\gamma(\mathbf{FIM}) = \det(\mathbf{FIM})$ in Eq. (8)), the compromise experiment, denoted as ξ_c, is found and defined as follows:

$$\xi_c = \underset{\xi \in \Xi}{\operatorname{argmin}} \left(\sum_{i=1}^{m} |\mathrm{D}(m_i, \xi_i^\star) - \mathrm{D}(m_i, \xi)|^p \right)^{1/p}. \tag{16}$$

Here, m represents the number of rival models, $\mathrm{D}(m_i, \xi)$ represents the value of the D-optimality design criterion for model m_i associated with experiment ξ, $\mathrm{D}(m_i, \xi_i^\star)$ represents the D-optimality design criterion value for model m_i associated with its corresponding D-optimal experiment ($\xi_i^\star$), and p is equal to 1, 2 or $+\infty$.

2.4.5. A note on model-robust designs

As mentioned in the Introduction of this paper, this problem was already tackled by Dette and Kwiecien (2004), who introduced the term model-robust designs. Their approach was developed for and evaluated using nested polynomial regression

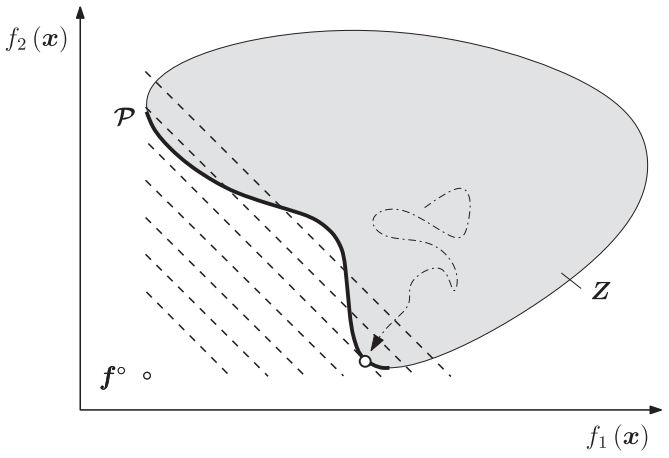

Fig. 4. Illustration of the ideal point ($\boldsymbol{f}^\circ$) method for a hypothetical multi-objective problem with two design variables ($\boldsymbol{x}_1$ and $\boldsymbol{x}_2$), where the aim is to simultaneously minimize two objective functions (f_1 and f_2) and where the ℓ_1 distance function is used.

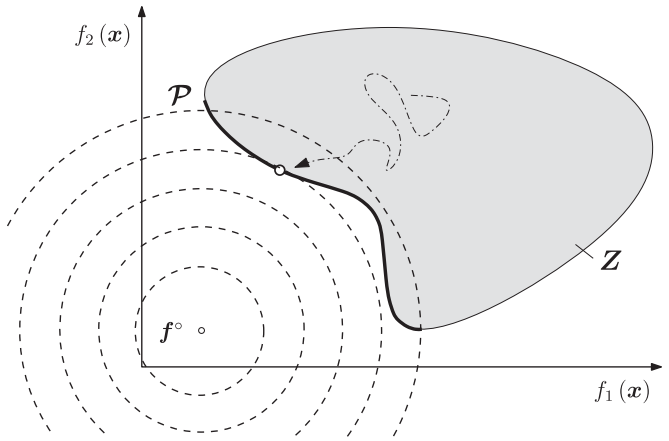

Fig. 5. Illustration of the ideal point ($\boldsymbol{f}^\circ$) method for a hypothetical multi-objective problem with two design variables ($\boldsymbol{x}_1$ and $\boldsymbol{x}_2$), where the aim is to simultaneously minimize two objective functions (f_1 and f_2) and where the ℓ_2 distance function is used.

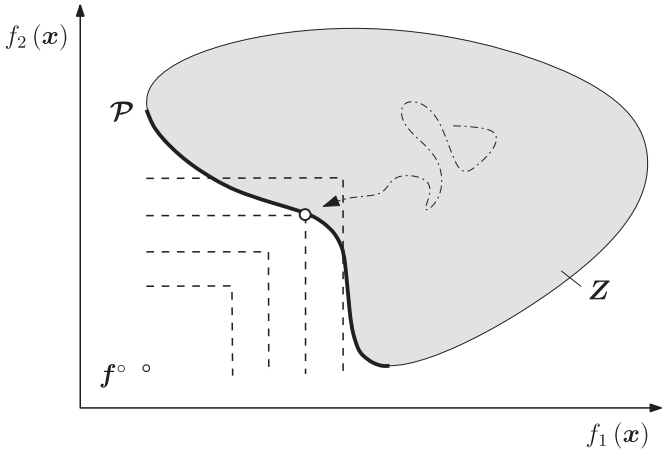

Fig. 6. Illustration of the ideal point ($\boldsymbol{f}^\circ$) method for a hypothetical multi-objective problem with two design variables ($\boldsymbol{x}_1$ and $\boldsymbol{x}_2$), where the aim is to simultaneously minimize two objective functions (f_1 and f_2) and where the ℓ_∞ distance function is used.

models that are linear in the model parameters. In their approach, the overall information content of the experiment with regard to the parameters of the rival models is evaluated using the geometric mean of the D-optimality design criterion values associated with the different models. So, following their rationale and using the notations introduced above, the model-robust design (or the compromise experiment) would be found after solving (Eq. (17)):

$$\xi_c = \underset{\xi \in \Xi}{\operatorname{argmax}} \prod_{i=1}^{m} \mathrm{D}(m_i, \xi)^{\lambda_i / n_{p_i}}, \tag{17}$$

where m represents the number of rival models and the quantities λ_i represent non-negative weights (with $\sum_{i=1}^{d} \lambda_i = 1$) reflecting the experimeter's prior belief in the adequacy of rival model m_i. An interesting feature of this approach is that the D-optimality design criterion values are scaled to account for the difference in the number of model parameters. Indeed, as explained in Section 2.3.3, the D-optimality design criterion is proportional to the volume of the confidence region of the parameter estimates and it is intuitively clear that the addition of an additional model parameter (or dimension) leads to a larger design criterion value. Although the possibility to account for this was not included in the ideal point method described in Section 2.4.4, modifying the ideal point method accordingly is straightforward and would be a very useful extension of the method.

2.5. Evaluating the capability to design a compromise experiment

Evaluating the presented method for its capability to design a compromise experiment is not a trivial task. The most intuitive approach would be to perform the compromise experiment as well as the optimal experiments, and compare the accuracy of the parameter estimates obtained after re-estimating them from each of the experiments. However, as discussed in Donckels et al. (2009b), this may give a biased picture of the method's performance when the models are nonlinear (which is for instance the case in the case study described below). If this is the case, the values of the design criteria depend on the parameter estimates (Atkinson and Donev, 1992; Ljung, 1999; Vanrolleghem and Van Daele, 1994; Vanrolleghem and Dochain, 1998; Walter and Pronzato, 1997), and these may change after performing the designed experiments and re-estimating the parameters. Note that this issue is inherent to optimal experimental design for nonlinear models, and is not restricted to the design of compromise experiments.

To evaluate the presented method on its capability to design a compromise experiment, the approach described in Donckels et al. (2009b) was also used here. Because the information content of an experiment is reflected by the value of the design criterion, the basis of the evaluation lies in the comparison of these criterion values. Since the ideal point method requires the design of an optimal experiment for each model, each of these optimal experiments can be performed instead of the compromise experiment. The information that is lost or gained when doing so is used for the evaluation. Note that, in this respect, it is important to realize that the information content or the quality of an experiment with regard to the parameters of a particular model can be compared to that of another experiment, but it is not meaningful to compare design criterion values from different models.

The information content of an experiment (ξ) with regard to the parameters of model m_i is represented by the corresponding D-optimality criterion value, denoted as $\mathrm{D}(m_i, \xi)$. These criterion values are calculated for each of the D-optimal experiments ($\xi_j^\star$, with $j = 1, \ldots, m$), and are compared to the criterion value associated with the compromise experiment (ξ_c). The ratio between these criterion values, denoted as $\Gamma_{\mathrm{D}_{ij}}$, is eventually used for the evaluation, and is calculated as

$$\Gamma_{\mathrm{D}_{ij}} = \frac{\mathrm{D}(m_i, \xi_c)}{\mathrm{D}(m_i, \xi_j^\star)}. \tag{18}$$

Since a higher information content is represented by a higher value of the D-optimality design criterion, it holds that $\Gamma_{\mathrm{D}_{ij}} > 1$ when the compromise experiment contains more information with regard to the parameters of model m_i than the optimal experiment for model m_j ($\xi_j^\star$). In other words, when $\Gamma_{\mathrm{D}_{ij}} > 1$, the estimates of the parameters of model m_i should be more accurate when the compromise experiment is performed instead of experiment $\xi_j^\star$.

2.6. Optimization algorithms

Both parameter estimation and optimal experimental design are optimization problems. To find the optimum, the use of optimization algorithms is required. In this work, the SIMPSA optimization algorithm proposed by Cardoso et al. (1996) was used. This algorithm combines the nonlinear simplex (Nelder and Mead, 1965) and the simulated annealing algorithm (Kirkpatrick et al., 1983). For more information on these optimization algorithms, the reader is referred to the cited papers.

3. Results and discussion

In this section, the experimental design concepts introduced in the previous section will be illustrated in a relatively simple case study, where nine models are proposed to describe the kinetic behavior of the enzyme glucokinase (*glk*, EC: 2.7.1.2). This enzyme catalyzes the conversion of glucose (GLU) and ATP to glucose-6-phosphate (G6P) and ADP, which is the first reaction of the glycolysis pathway.

In this case study, a compromise experiment will be designed for three scenarios: optimization of the sampling times, optimization of the initial conditions of the experiment, and optimization of both the sampling times and the initial conditions. With these examples, a number of research questions are addressed. First of all, the case study should demonstrate the capability or incapability of the ideal point method to design compromise experiments. In addition, it should indicate whether the choice of the distance function (ℓ_1, ℓ_2 and ℓ_∞) matters, and, if so, which of these metrics is preferred. Finally, it would be interesting to compare the performance of the ideal point method to that of the kernel-based method presented in Donckels et al. (2009b), where possible.

3.1. General model

Before describing the different kinetics, a general model for the enzymatic conversion process is formulated. For this, it is assumed that the experimental setup allows one to give a pulse of glucose, ATP and PEP, or a mixture thereof.

The volume of the reaction vessel, denoted as V[L], is determined by the flow rate of the pulse, denoted as F_p [L/s], and by the sampling volume and frequency. However, in this example, the sampling volume will be neglected and the volume can thus be described by

$$\frac{d\mathrm{V}}{dt} = F_p. \tag{19}$$

For the concentration of glucokinase, denoted as GLK [mg/L], only a dilution effect is considered, and inactivation of the enzyme

is thus neglected. Given the fact that a typical experiment ends after 20 min, this is a reasonable assumption. The resulting equation for describing the enzyme concentration is given as

$$\frac{d\mathrm{GLK}}{dt} = -\frac{F_p}{\mathrm{V}} \cdot \mathrm{GLK}. \tag{20}$$

The equations used to describe the other state variables (all of which are expressed in mM) are given as

$$\frac{d\mathrm{GLU}}{dt} = \frac{F_p}{\mathrm{V}} \cdot (\mathrm{GLU}_p - \mathrm{GLU}) - v_{glk}, \tag{21}$$

$$\frac{d\mathrm{ATP}}{dt} = \frac{F_p}{\mathrm{V}} \cdot (\mathrm{ATP}_p - \mathrm{ATP}) - v_{glk}, \tag{22}$$

$$\frac{d\mathrm{G6P}}{dt} = -\frac{F_p}{\mathrm{V}} \cdot \mathrm{G6P} + v_{glk}, \tag{23}$$

$$\frac{d\mathrm{ADP}}{dt} = -\frac{F_p}{\mathrm{V}} \cdot \mathrm{ADP} + v_{glk}, \tag{24}$$

$$\frac{d\mathrm{PEP}}{dt} = \frac{F_p}{\mathrm{V}} \cdot (\mathrm{PEP}_p - \mathrm{PEP}). \tag{25}$$

Here, GLU_p, ATP_p and PEP_p represent the concentrations [mM] of glucose, ATP and PEP in the pulse, respectively, and v_{glk} represents the velocity equation describing the kinetic behavior of glucokinase [mM/s].

3.2. Rival models

The conversion catalyzed by glucokinase is a bi-reactant system (Segel, 1975). Two reaction mechanisms are possible for such a system: random and ordered. In a random bi-reactant system, the order in which the two substrates bind does not matter, whereas in an ordered bi-reactant system one of the substrates has to bind to the enzyme first, before the second substrate can bind and the reaction can take place. In addition, it was recently suggested that glucokinase may be inhibited by phosphoenolpyruvate (PEP) (Ogawa et al., 2007).

Based on these considerations, nine models were defined to describe the enzyme kinetics (Segel, 1975). The models differ in the equation used to describe the enzyme kinetics, each of which is based on a particular hypothesis of how the enzyme works. Although the kinetic equation is different for each rival model, each one is of the following form:

$$v_{glk} = k \cdot \mathrm{GLK} \cdot \frac{\dfrac{\mathrm{GLU}}{K_{GLU}} \cdot \dfrac{\mathrm{ATP}}{K_{ATP}}}{\varphi_i(\mathrm{GLU}, \mathrm{ATP}, \mathrm{PEP})}, \tag{26}$$

where the parameter k expresses the maximum specific reaction rate [U/mg], where one unit is defined as that amount of enzyme that catalyzes one μmol of substrate in 1 min. The part that is different for each rival model m_i is represented by $\varphi_i(\mathrm{GLU}, \mathrm{ATP}, \mathrm{PEP})$.

For models m_1, m_2 and m_3, it is assumed that the reaction mechanism is random. With regard to the inhibition by PEP, three scenarios are possible (also for the other models described further on): there is no inhibition by PEP (Eq. (27)), PEP inhibits the binding of ATP (Eq. (28)) and PEP inhibits the binding of glucose (Eq. (29)). This results in the following equations:

$$\varphi_1(\mathrm{GLU}, \mathrm{ATP}, \mathrm{PEP}) = 1 + \frac{\mathrm{GLU}}{K_{GLU}} + \frac{\mathrm{ATP}}{K_{ATP}} + \frac{\mathrm{GLU}}{K_{GLU}} \cdot \frac{\mathrm{ATP}}{K_{ATP}}, \tag{27}$$

$$\varphi_2(\mathrm{GLU}, \mathrm{ATP}, \mathrm{PEP}) = 1 + \frac{\mathrm{GLU}}{K_{GLU}} + \frac{\mathrm{ATP}}{K_{ATP}} + \frac{\mathrm{PEP}}{K_{PEP}} + \frac{\mathrm{GLU}}{K_{GLU}} \cdot \frac{\mathrm{PEP}}{K_{PEP}} + \frac{\mathrm{GLU}}{K_{GLU}} \cdot \frac{\mathrm{ATP}}{K_{ATP}}, \tag{28}$$

$$\varphi_3(\mathrm{GLU}, \mathrm{ATP}, \mathrm{PEP}) = 1 + \frac{\mathrm{GLU}}{K_{GLU}} + \frac{\mathrm{ATP}}{K_{ATP}} + \frac{\mathrm{PEP}}{K_{PEP}} + \frac{\mathrm{ATP}}{K_{ATP}} \cdot \frac{\mathrm{PEP}}{K_{PEP}} + \frac{\mathrm{GLU}}{K_{GLU}} \cdot \frac{\mathrm{ATP}}{K_{ATP}}. \tag{29}$$

For the other six models, an ordered reaction mechanism is assumed. For models m_4, m_5 and m_6, it is assumed that glucose is the first binding substrate, which results in the following equations:

$$\varphi_4(\mathrm{GLU}, \mathrm{ATP}, \mathrm{PEP}) = 1 + \frac{\mathrm{GLU}}{K_{GLU}} + \frac{\mathrm{GLU}}{K_{GLU}} \cdot \frac{\mathrm{ATP}}{K_{ATP}}, \tag{30}$$

$$\varphi_5(\mathrm{GLU}, \mathrm{ATP}, \mathrm{PEP}) = 1 + \frac{\mathrm{GLU}}{K_{GLU}} + \frac{\mathrm{GLU}}{K_{GLU}} \cdot \frac{\mathrm{PEP}}{K_{PEP}} + \frac{\mathrm{GLU}}{K_{GLU}} \cdot \frac{\mathrm{ATP}}{K_{ATP}}, \tag{31}$$

$$\varphi_6(\mathrm{GLU}, \mathrm{ATP}, \mathrm{PEP}) = 1 + \frac{\mathrm{GLU}}{K_{GLU}} + \frac{\mathrm{ATP}}{K_{ATP}} \cdot \frac{\mathrm{PEP}}{K_{PEP}} + \frac{\mathrm{GLU}}{K_{GLU}} \cdot \frac{\mathrm{ATP}}{K_{ATP}}. \tag{32}$$

The equations associated with models m_7, m_8 and m_9 are similar, but ATP is assumed to be the first binding substrate. The equations for the corresponding models are

$$\varphi_7(\mathrm{GLU}, \mathrm{ATP}, \mathrm{PEP}) = 1 + \frac{\mathrm{ATP}}{K_{ATP}} + \frac{\mathrm{GLU}}{K_{GLU}} \cdot \frac{\mathrm{ATP}}{K_{ATP}}, \tag{33}$$

$$\varphi_8(\mathrm{GLU}, \mathrm{ATP}, \mathrm{PEP}) = 1 + \frac{\mathrm{ATP}}{K_{ATP}} + \frac{\mathrm{GLU}}{K_{GLU}} \cdot \frac{\mathrm{PEP}}{K_{PEP}} + \frac{\mathrm{GLU}}{K_{GLU}} \cdot \frac{\mathrm{ATP}}{K_{ATP}}, \tag{34}$$

$$\varphi_9(\mathrm{GLU}, \mathrm{ATP}, \mathrm{PEP}) = 1 + \frac{\mathrm{ATP}}{K_{ATP}} + \frac{\mathrm{ATP}}{K_{ATP}} \cdot \frac{\mathrm{PEP}}{K_{PEP}} + \frac{\mathrm{GLU}}{K_{GLU}} \cdot \frac{\mathrm{ATP}}{K_{ATP}}. \tag{35}$$

3.3. Real model and data generation

According to literature (Monasterio and Cárdenas, 2003; Ogawa et al., 2007), the reaction mechanism of glucokinase is ordered, with glucose as first binding substrate, and PEP inhibiting the binding of ATP to the enzyme. Based on these considerations, the fifth model was chosen as the real or *true* model (m_5^*). This model was used to generate experimental data by simulating the experiment using the parameter values tabulated in Table 1, and by adding random noise to mimic the measurement error. The standard deviations of the measurements were calculated in the same way as suggested by Ternbach et al. (2005):

$$\sigma_y = \hat{y} \cdot \varsigma_y \cdot \left(1 + \frac{1}{\left(\dfrac{\hat{y}}{lb_y}\right)^2 + \dfrac{\hat{y}}{lb_y}} \right). \tag{36}$$

Here, ς_y represents a constant minimal relative error, and lb_y represents the lower accuracy bound on the measurement of y. In this way, the standard deviation of the measurements is proportional to the value of $\hat{y}$, but increases when the latter approaches the lower accuracy bound on the measurement. Note that these σ_y-values are used to construct the measurement error covariance matrix, denoted as $\boldsymbol{\Sigma}$ (see Section 2.2), which is assumed here to be a diagonal matrix. As the diagonal elements of this matrix represent the variances of the measurements, they can be calculated as σ_y^2.

3.4. Preliminary experiment

To initiate the case study, a preliminary experiment was defined and performed *in silico*. For this experiment, the volume of the reaction vessel was set to 10 mL, and the initial glucokinase concentration was set such that 5 units were present in the reaction

Table 1
Parameters of the real model (m_5^*) that were used to generate experimental data, the parameter estimates obtained after fitting the rival models to the data from the preliminary experiment, as well as the corresponding 95% confidence intervals and WSSE- values.

model	k	K_{GLU}	K_{ATP}	K_{PEP}	WSSE
m_5^*	312	0.15	0.13	0.10	–
m_1	314.13 ± 90.48	0.0173 ± 0.1135	0.1407 ± 0.0694	–	61.5287
m_2	336.14 ± 107.66	0.0451 ± 0.1341	0.1533 ± 0.0772	0.1466 ± 0.2198	57.1080
m_3	317.21 ± 93.38	0.0191 ± 0.1162	0.1412 ± 0.0705	0.0091 ± 0.0544	56.9125
m_4	307.64 ± 49.17	0.1299 ± 0.8481	0.1245 ± 0.0441	–	61.2821
m_5	312.41 ± 51.28	0.2011 ± 0.9320	0.1207 ± 0.0461	0.1261 ± 0.2145	56.9285
m_6	319.87 ± 55.23	0.3112 ± 1.0616	0.1182 ± 0.0491	0.1076 ± 0.3577	57.1491
m_7	412.58 ± 180.30	0.0099 ± 0.1706	27.9603 ± 464.53	–	94.2223
m_8	428.11 ± 236.59	0.0148 ± 0.2146	19.4047 ± 265.68	8.7458 ± 127.33	77.5805
m_9	543.60 ± 438.34	0.1102 ± 0.3893	3.6812 ± 9.2598	0.0127 ± 0.0327	88.2185

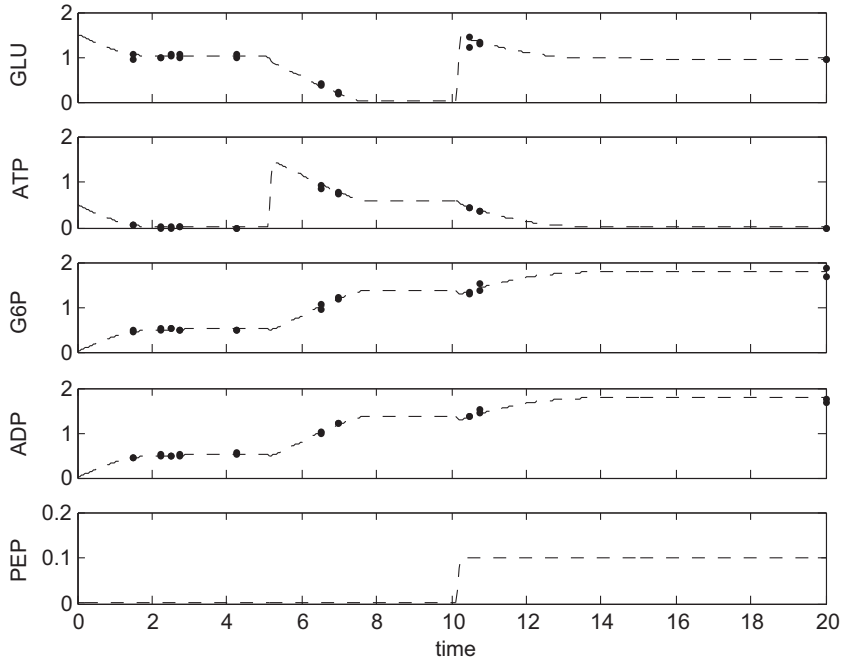

Fig. 7. Preliminary experiment simulated with the real model (m_5^*) (- -), and the experimental data (•) obtained from it.

mixture. Further, it was assumed that no G6P, ADP and PEP were present at the start of the experiment, and the initial concentrations of glucose and ATP were set to 1.5 and 0.5 mM, respectively.

During the experiment, two pulses were given, for both of which the volume was equal to 1 mL. The first pulse was given 5 min after the start of the experiment, and only contained ATP. The ATP concentration was chosen such that the ATP concentration in the reaction mixture was raised to 1.5 mM. The second pulse, given 10 min after the start of the experiment, contained glucose and PEP, and their concentrations were chosen such that the resulting concentrations in the reaction mixture were 1.5 and 0.1 mM, respectively.

The experiment was stopped after 20 min, and 10 measurements of GLU, ATP, G6P and ADP were taken in duplicate (see Fig. 7). The minimal relative errors (ς) were arbitrarily set to 0.05 for all measured state variables, and the lower accuracy bounds on the measurements were defined as 0.1 mM.

3.5. Parameter estimation

The parameters of all rival models were estimated using the data from this preliminary experiment (Fig. 7), and using the optimization algorithm described in Section 2.6. Since negative parameter values do not make sense, the lower bounds were set to zero. The upper bounds were set to 1000 U/mg for parameter k, 2 mM for parameter K_{GLU}, 50 mM for parameter K_{ATP}, and 25 mM for parameter K_{PEP}. The results of this parameter estimation exercise are shown in Table 1. From these results, one can conclude that the accuracy of the parameter estimates is quite low, indicating that it may be beneficial to perform a compromise experiment to increase the accuracy of the parameter estimates prior to the start of the model discrimination procedure.

3.6. Optimization of sampling times

This section describes the results for the scenario in which 10 sampling times were optimized. The initial concentrations and the characteristics of the two pulses that are given during the course of the experiment are fixed to the ones of the preliminary experiment. Further, it is assumed that a minimum time interval of 15 s is required by the experimental setup between two subsequent sampling times. To clearly illustrate the different steps of the ideal point method, the results of this scenario will be discussed in more detail than the ones for the other scenarios. In addition, they will be compared to those presented in Donckels et al. (2009b), where a kernel-based method was applied to the same case study.

The compromise experiment is found after minimizing the distance between the ideal point and the point in criterion space that corresponds with the experiment being proposed by the optimization algorithm (as explained in Section 2.4.3). Obviously, the ideal point has to be determined first. For this purpose, an experiment is designed for each of the rival models by optimizing the D-optimality design criterion (Eq. (13)). The results of these (nine) experimental design exercises are shown in Fig. 8.

Once the ideal point is determined, the compromise experiment is found by applying the optimization algorithm described in Section 2.6 to solve the optimization problem formalized in Eq. (16). This optimization exercise is done for each of the three distance functions described earlier (ℓ_1, ℓ_2 and ℓ_∞). The resulting compromise sampling times are shown in Fig. 9 as well as the compromise sampling times found using the kernel-based method (Donckels et al., 2009b). From these results, one can see that, except for the ℓ_∞ distance function, the compromise sampling times are similar for the different methods.

To evaluate the capability of the presented method to design a compromise experiment, the approach outlined in Section 2.5 is adopted. For this purpose, the $\Gamma_{D_{i1}}$- values are calculated from Eq. (18) and presented as a barplot (see Fig. 10). For each model m_i, the value of $\Gamma_{D_{i1}}$ is represented by the black bar ($\xi_1^\star$), and the bars become increasingly white as the model number increases ($\xi_1^\star \rightarrow \xi_9^\star$). When $\Gamma_{D_{ij}} > 1$, the estimates of the parameters of model m_i should be more accurate when the compromise experiment is performed instead of experiment $\xi_j^\star$. To present the results in a systematic and easily interpretable form, the values of $\Gamma_{D_{ij}}$ are represented on a logarithmic scale. In this way, it is easy to see when $\Gamma_{D_{ij}} > 1$.

For brevity, the results of this evaluation will only be discussed in detail for the case where the ℓ_2 distance function was used. The results are shown in Fig. 10, and clearly illustrate the ability of the presented method to design an experiment with the characteristics of a compromise experiment. For instance, the $\Gamma_{D_{i1}}$- values for model m_1 show that $\Gamma_{D_{1j}} < 1$ for experiments $\xi_1^\star$, $\xi_3^\star$ and $\xi_4^\star$, which indicates that these experiments contain more information with regard to the parameters of model m_1 than the compromise experiment. For the other optimal experiments, this is not the case and the compromise experiment is preferred. If one would perform $\xi_4^\star$ instead of the compromise experiment, the information content would indeed be higher for model m_1, but it would be lower for the other models (except for model m_4, of course). The latter can be seen when comparing the bars corresponding to $\xi_4^\star$ for the different models. That the compromise experiment is not optimal for the individual models is a direct result of the fact

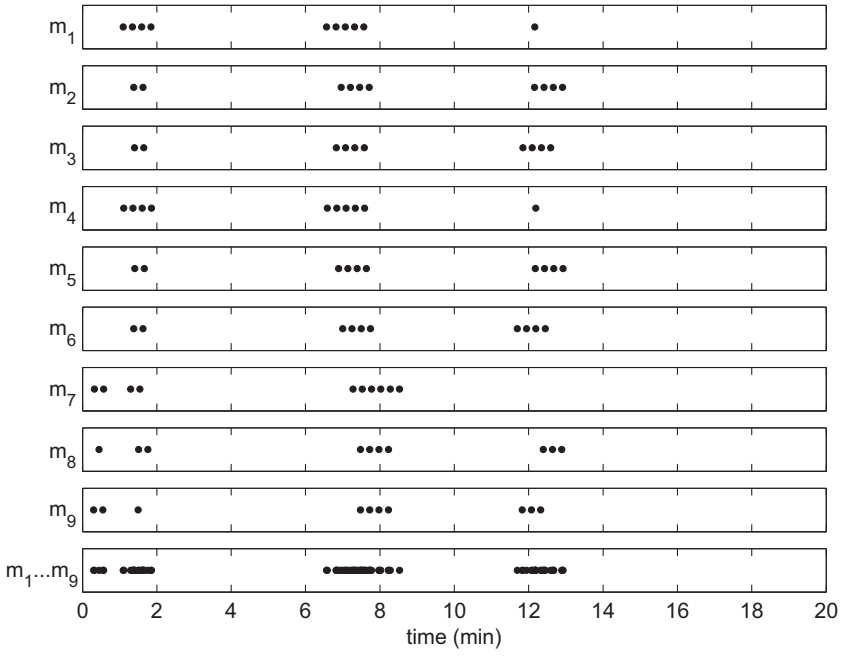

Fig. 8. Optimal sampling times (•) found for the nine rival models for the case where the D-optimality design criterion was optimized by varying the sampling times. The graph at the bottom was obtained by plotting the 10 optimal sampling times of the nine individual models on the same axis.

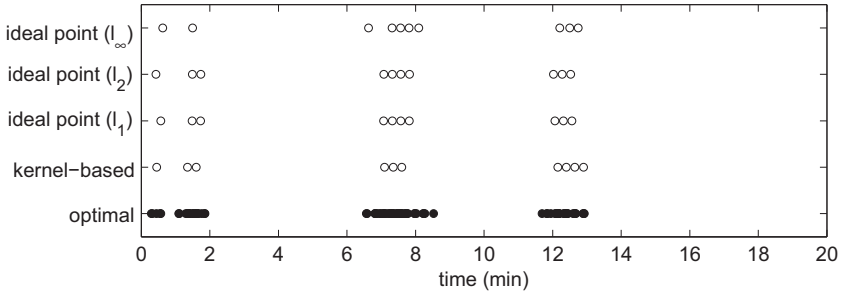

Fig. 9. Optimal sampling times for the individual models (•) and the compromise sampling times (◦) found using the kernel-based method, and the ideal point method using the different distance functions (ℓ_1, ℓ_2 and ℓ_∞).

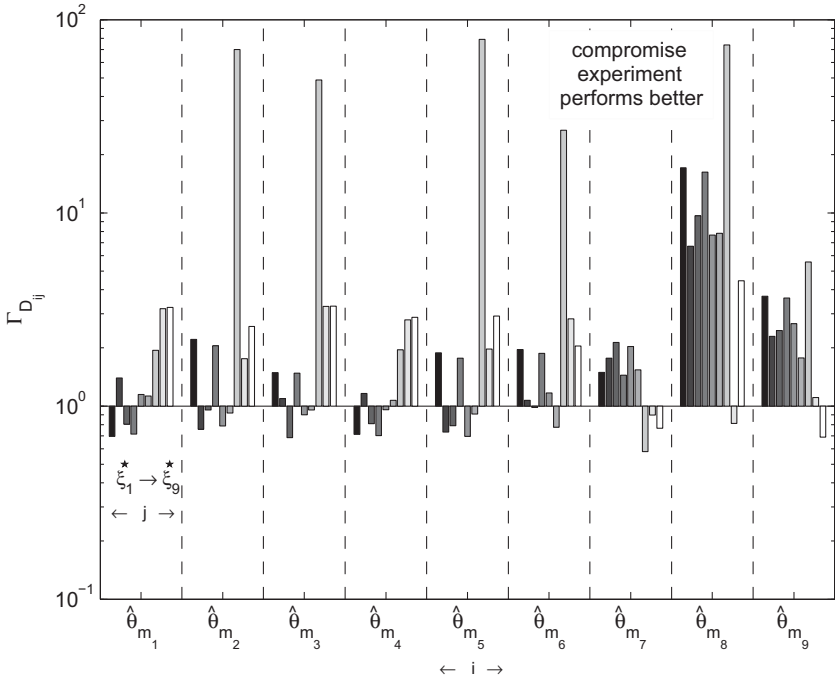

Fig. 10. $\Gamma_{D_{ij}}$- values for the scenario in which the sampling times are optimized and where the ℓ_2 distance function is used. The black bars correspond to the optimal experiments associated with model m_1, and the bars become increasingly white as the model number increases.

that the optimal sampling times are different for the individual models (see Fig. 8). Yet, the compromise experiment seems to be sufficiently informative to improve the overall accuracy of the parameter estimates.

Another interesting observation can be made from the results for the parameters of models m_7, m_8 and m_9. Apparently, each of the D-optimal experiments of the other models is significantly less informative with regard to their parameters compared to the compromise experiment, which performs quite well. This indicates that one or more compromise sampling times that are not present in the D-optimal experiments contain a lot of information on the parameters of those models. Indeed, from Fig. 8 one can see that the D-optimal experiments for models m_7, m_8 and m_9 have one or two sampling times around 0.5 min, while this is not the case for models m_1 till m_6. Because one of the compromise sampling times is located in this time range (as shown in Fig. 9), the compromise experiment performs significantly better for these models (m_7, m_8 and m_9) than the D-optimal experiments from the other models. In addition, one can see that the D-optimal experiments for models m_7 and m_9 have two sampling times at about 0.5 min, while the D-optimal experiment for model m_8 and the compromise experiment have only one. This explains why this phenomenon is less pronounced for models m_7 and m_9.

To evaluate the results obtained with the other distance functions, the values of $\Gamma_{D_{ij}}$ were calculated as well, but to facilitate the comparison between the distance functions, these values are presented in one figure using boxplots (Fig. 11). On each box, the central mark represents the median, the edges of the box represent the 25th and 75th percentiles, the whiskers extend to the most extreme data points not considered outliers, and outliers are plotted individually (the crosses). By presenting the $\Gamma_{D_{ij}}$- values in this way, information is lost on which of the D-optimal experiments performs better or worse than the compromise experiment for the individual models, but this information is not essential for this purpose. In fact, the median is of great importance. If the median is above one, it indicates that the compromise experiment performs better than the majority of the D-optimal experiments.

That it is possible to design a compromise experiment using the ℓ_2 distance function can of course be concluded from these boxplots as well. This is especially clear from the medians (indicated by the horizontal lines in the box) which are always larger than one, but also from the fact that a larger part of the box is above this level. So, for each of the rival models, the compromise experiment performs better than the majority of the D-optimal experiments, which is in accordance with the required characteristics of a compromise experiment.

From Fig. 11, one can also observe that the results obtained with the ℓ_1 distance function are very similar to the ones obtained with the ℓ_2 distance function, which is not surprising given the fact that the compromise sampling times are nearly identical (Fig. 8). Indeed, situations can occur where the Pareto front is such that the solutions obtained with the different distance functions are the same. Although this is not the case for the hypothetical Pareto front shown in Figs. 4, 5 and 6, it would for instance be the case when the Pareto front looks like the one shown in Fig. 3.

For the ℓ_∞ distance function, the compromise sampling times are slightly different. This is also reflected in the values of $\Gamma_{D_{ij}}$, from which one can conclude that the majority of the D-optimal experiments perform slightly better than the designed compromise experiment for models m_1 to m_6. For models m_7, m_8 and m_9, which are the models where ATP is the first binding substrate and for which the model structures resemble each other, this is not the case. This suggests that for this example the ℓ_∞ distance function may not be the most suitable one to design a compromise experiment.

For illustratory purposes, the parameter estimates and the uncertainty thereon obtained after performing the individual D-optimal experiments and the compromise experiment (obtained using the ℓ_2 distance function) are shown in Table 2. Note that these parameter estimates were obtained after re-estimating the model parameters using the newly collected experimental data.

To conclude this section, the results obtained using the ideal point method are compared to the ones obtained with the kernel-based method presented in Donckels et al. (2009b) and briefly described in Section 2.4.1. Although the compromise sampling

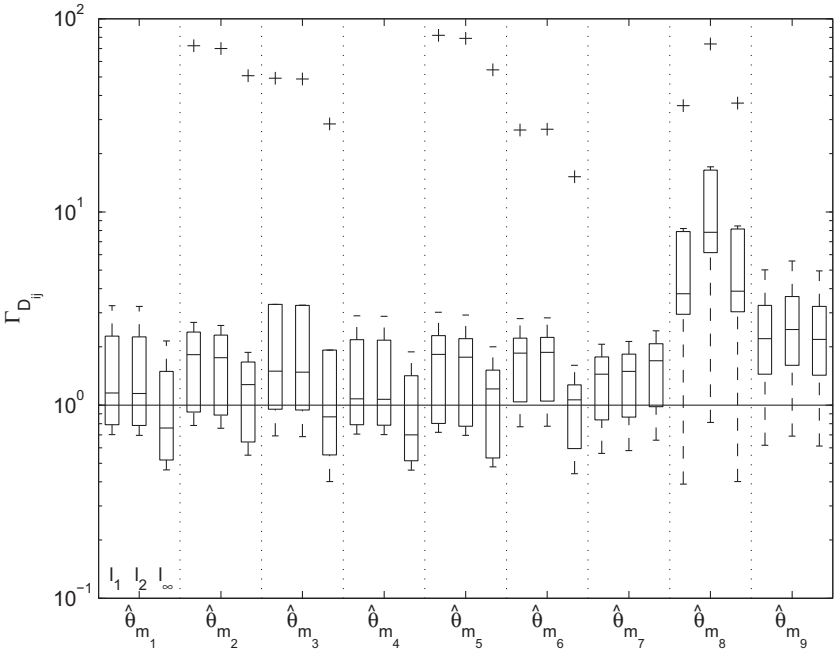

Fig. 11. $\Gamma_{D_{ij}}$- values for the scenario in which the sampling times are optimized, and where the ℓ_1, ℓ_2 and ℓ_∞ distance functions are used.

Table 2
Parameters of the real model ($m_5^\star$) that were used to generate experimental data, and the parameter estimates obtained after fitting model m_5 to the data from both the preliminary experiment (denoted here as ξ_p) and the individual D-optimal experiments or the compromise experiment (ξ_c), together with the 95% confidence intervals and the corresponding WSSE- values.

Model	k	K_{GLU}	K_{ATP}	K_{PEP}	WSSE
$m_5^\star$	312	0.15	0.13	0.10	–
ξ_p	312.41 ± 51.28	0.2011 ± 0.9320	0.1207 ± 0.0461	0.1261 ± 0.2145	56.9285
ξ_c	311.64 ± 13.23	0.1665 ± 0.0975	0.1239 ± 0.0164	0.0854 ± 0.0198	145.7474
$\xi_1^\star$	309.01 ± 11.10	0.1278 ± 0.0798	0.1301 ± 0.0142	0.1046 ± 0.0339	129.4858
$\xi_2^\star$	316.69 ± 13.80	0.1728 ± 0.0960	0.1351 ± 0.0173	0.1080 ± 0.0257	132.3969
$\xi_3^\star$	306.19 ± 11.33	0.1207 ± 0.0818	0.1256 ± 0.0159	0.1033 ± 0.0245	152.1429
$\xi_4^\star$	314.03 ± 12.15	0.1739 ± 0.0921	0.1306 ± 0.0146	0.0772 ± 0.0211	147.6936
$\xi_5^\star$	309.98 ± 12.06	0.1369 ± 0.0893	0.1264 ± 0.0162	0.0945 ± 0.0213	144.1867
$\xi_6^\star$	313.61 ± 13.68	0.1685 ± 0.1001	0.1277 ± 0.0168	0.1085 ± 0.0277	147.0389
$\xi_7^\star$	311.91 ± 15.21	0.1672 ± 0.1016	0.1236 ± 0.0172	0.1469 ± 0.2538	118.3752
$\xi_8^\star$	312.01 ± 16.82	0.1466 ± 0.1014	0.1312 ± 0.0179	0.1051 ± 0.0257	126.9117
$\xi_9^\star$	309.42 ± 16.91	0.1295 ± 0.1009	0.1266 ± 0.0199	0.0950 ± 0.0252	125.5086

times obtained with these methods are not identical (as shown in Fig. 9), the $\Gamma_{D_{ij}}$- values are very similar. From these results, which were not reproduced here for brevity, one can conclude that the considered methods perform equally well for experimental design exercises where only the sampling times are optimized. Note, however, that the ideal point method is computationally more demanding, because next to the optimizations required to determine the ideal point, one additional optimization is needed to solve Eq. (16). This is not necessary when the kernel-based method is used, where the compromise sampling times are directly calculated from the optimal sampling times.

3.7. Optimization of initial conditions

This section describes the results for the scenario in which the sampling times and the manipulations (the pulses) were fixed to the ones from the preliminary experiment, but the initial concentrations of glucose, ATP and PEP were optimized. For this, the lower bounds were set to 0 mM, and the upper bounds to 2 mM.

The optimal values for the initial concentrations are shown in Fig. 12. Because both the characteristics of the two pulses (timing and concentrations of glucose, ATP and PEP) and the sampling times are fixed, the initial conditions are chosen such that the information with regard to the parameters of the individual models is maximal at the given sampling times. This explains why, in contrast to the optimal experiments found in the previous scenario, the optimal experiments are very different for the individual rival models.

Based on the D-optimal criterion values associated with these optimal experiments, the ideal point was defined and a compromise experiment was designed using the three distance functions described above. In Fig. 12, the initial concentrations from the obtained compromise experiments are compared to the initial concentrations from the D-optimal experiments of the rival models. One can clearly see that the compromise experiments found using the ℓ_1 and ℓ_2 distance function are very similar, while a different experiment is found with the ℓ_∞ distance function.

The similarity between the compromise experiments found using the ℓ_2 and the ℓ_1 distance function is obviously reflected in

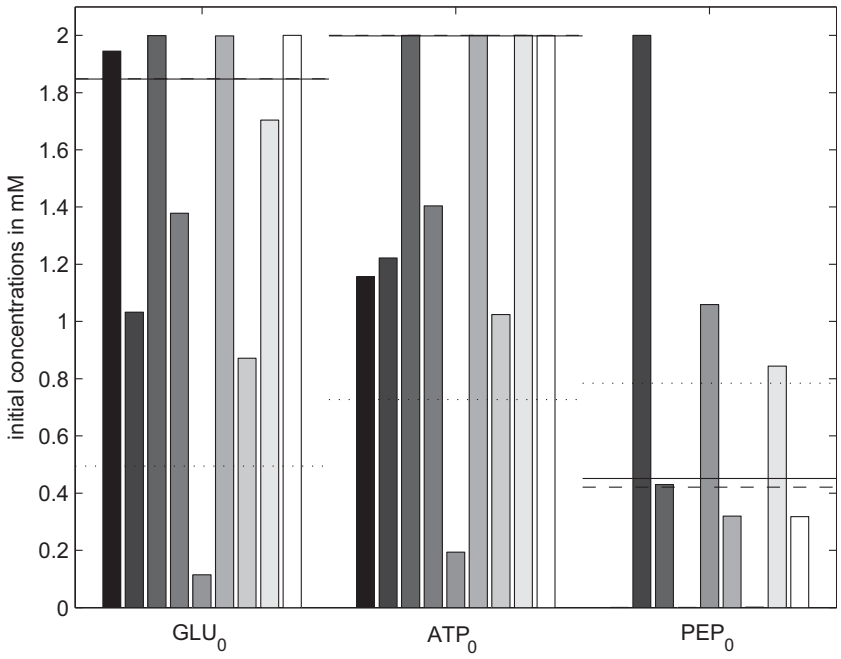

Fig. 12. Initial concentrations of glucose, ATP and PEP associated with the D-optimal experiments of the rival models (m_1 corresponds to the black bar, and the bars become increasingly white as the model number increases), as well as those associated with the compromise experiment found using the ideal point method (horizontal lines) after using the ℓ_1 (– –), the ℓ_2 (—) and the ℓ_∞ (···) distance function. Note that the lines for ℓ_1 and ℓ_2 overlap for GLU_0 and ATP_0.

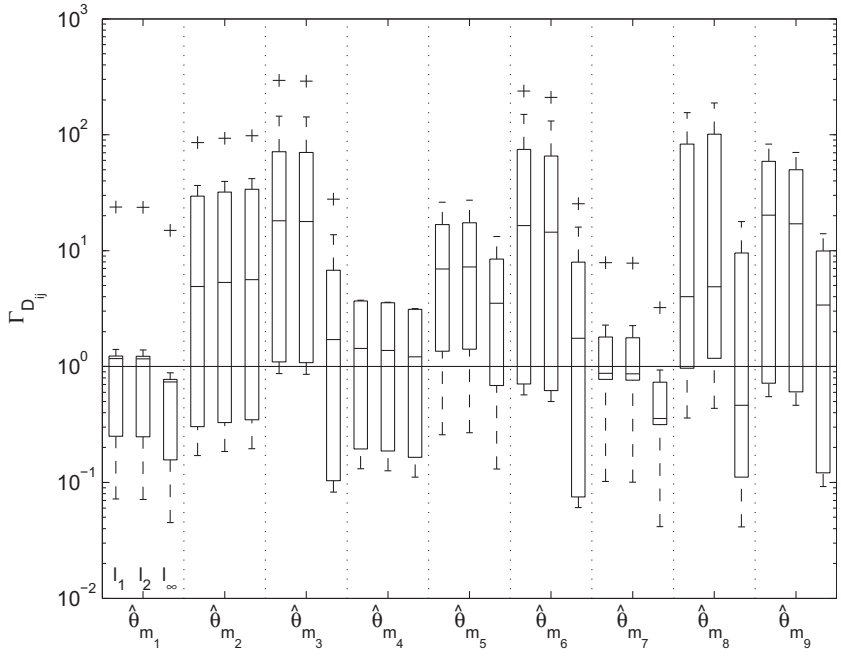

Fig. 13. $\Gamma_{D_{ij}}$- values for the scenario in which the initial conditions are optimized, and where the ℓ_1, ℓ_2 and ℓ_∞ distance functions are used..

the $\Gamma_{D_{ij}}$- values, shown in Fig. 13. For both cases, the boxplots indicate that the majority of these values are larger than one, indicating that it is advisable to perform the compromise experiment instead of the corresponding D-optimal experiments. However, for the case where the ℓ_∞ distance function is used, the barplots indicate that, although the majority of the medians is larger than one, some of the $\Gamma_{D_{ij}}$- values are significantly lower (for instance, for models m_1, m_3, m_6 and m_7). In conclusion, one can state that also for this scenario, the ℓ_∞ distance function seems to be the least suitable one.

3.8. Optimization of initial conditions and sampling times

The scenario in which both the sampling times and the initial conditions were optimized is described in this section. As in the previous scenarios, the initial conditions were allowed to take values between 0 and 2 mM, 10 samples were taken and the minimum time between two samples was set to 15 s.

The D-optimal experiments and the compromise experiments found using the ℓ_1, ℓ_2 and ℓ_∞ distance functions are represented in Figs. 14, 15 and 16. These results indicate that, as more

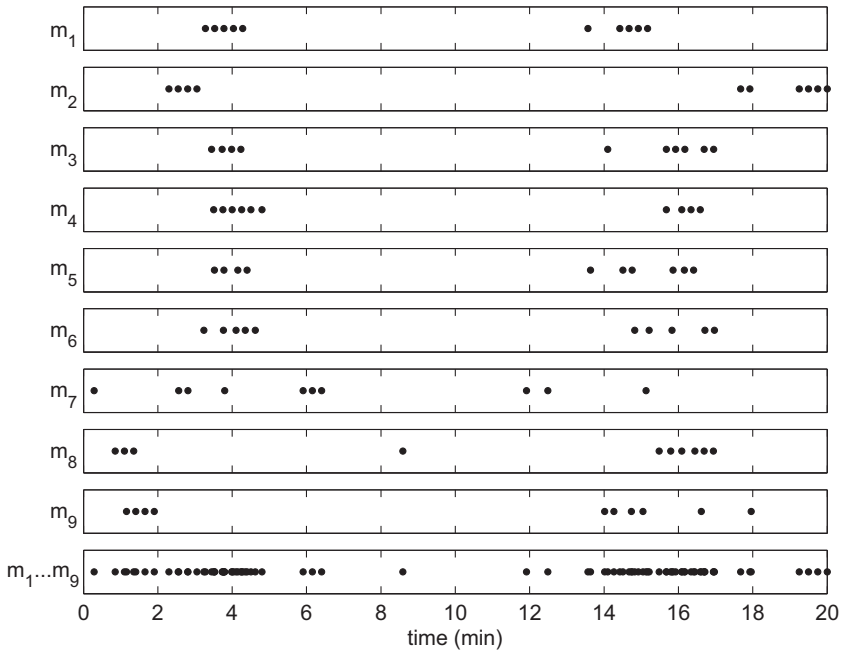

Fig. 14. Optimal sampling times (•) found for the nine rival models for the case where the D-optimality design criterion was optimized by varying both the sampling times and the initial concentrations of glucose, ATP and PEP. The graph at the bottom was obtained by plotting the 10 optimal sampling times of the nine individual models on the same axis.

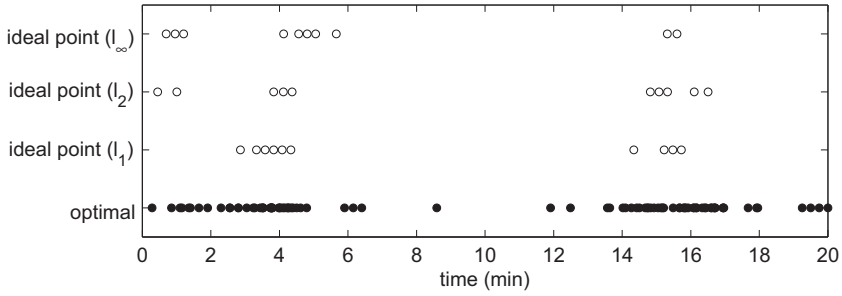

Fig. 15. Optimal sampling times for the individual models (•) and the compromise sampling times (◦) found using the ideal point method using the different distance functions (ℓ_1, ℓ_2 and ℓ_∞).

experimental degrees of freedom become available, the D-optimal experiments become more and more specific for the individual models. This is especially clear when considering the optimal sampling times shown in Fig. 14. This specificity obviously makes the design of a compromise experiment more challenging.

From the $\Gamma_{D_{ij}}$- values shown in Fig. 17, one can conclude that also for this scenario a compromise experiment is found when the ℓ_2 distance function is used. However, the values of $\Gamma_{D_{ij}}$ obtained for the two other distance functions are systematically smaller than the ones obtained with the ℓ_2 distance function. In addition, for several models, the medians are smaller than one. This means that for the majority of the D-optimal experiments more accurate parameter estimates can be obtained than if the designed compromise experiment would be performed. This indicates that the characteristics of the experiments designed using the ℓ_1 and ℓ_∞ distance functions are not consistent with the ones of a compromise experiment.

To conclude this section, the reader is pointed to the fact that the specificity discussed above can also be observed from the $\Gamma_{D_{ij}}$- values shown in Fig. 17. These $\Gamma_{D_{ij}}$- values are generally larger than the ones obtained in the other scenarios (Figs. 11 and 13) and the variation among these values is much higher. This indicates that for some models, a significant amount of information on its parameters can be lost when performing an optimal experiment for another model instead of the compromise experiment. In other words, an optimal experiment for one model is often all but optimal for another one.

3.9. Further discussion of the performance of the distance functions

From the results and discussion above, one can conclude that the ℓ_2 distance function is the preferred one for this case study. However, the fact that the ℓ_1 distance functions performed well in the first two scenarios but was not the best option in the third scenario, indicates that the performance of a particular distance function is case specific. Indeed, the performance of the distance function depends on the shape of the Pareto front, which, unfortunately, cannot be clearly visualized for multi-objective problems with more than three objectives. Nevertheless, when the ideal point method is applied in another case study, the approach used here to evaluate the capability to design a

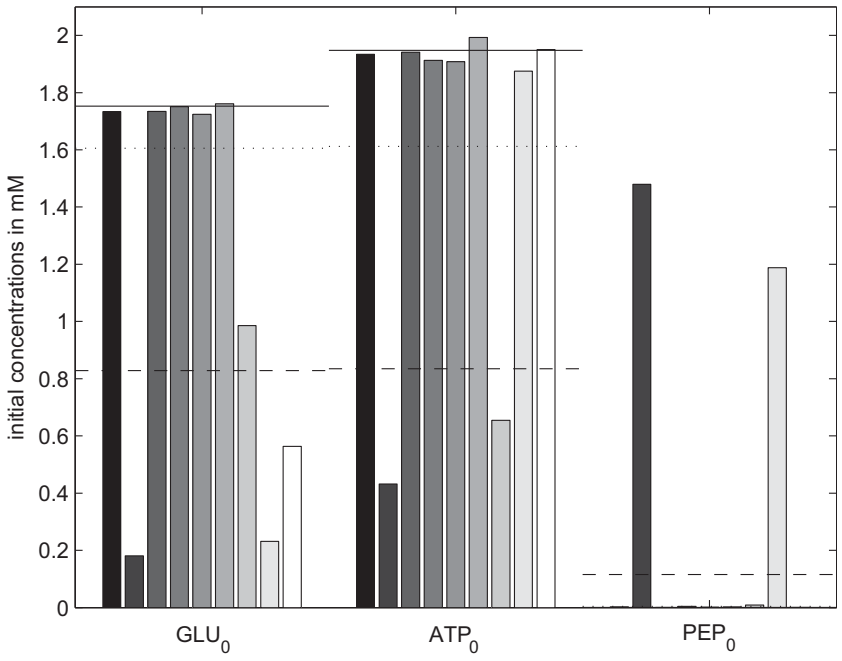

Fig. 16. Initial concentrations of glucose, ATP and PEP associated with the D-optimal experiments of the rival models (m_1 corresponds to the black bar, and the bars become increasingly white as the model number increases), as well as those associated with the compromise experiment found using the ideal point method (horizontal lines) after using the ℓ_1 (– –), the ℓ_2 (—) and the ℓ_∞ (···) distance function. Note that for several models the values of PEP_0 are zero, as well as those associated with the compromise experiments found using the ℓ_2 and ℓ_∞ distance functions.

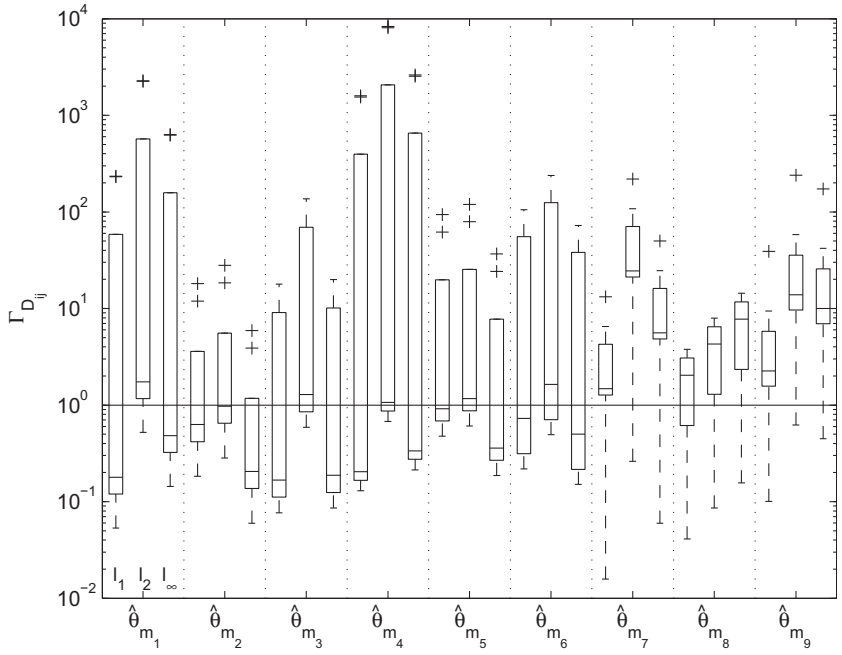

Fig. 17. $\Gamma_{D_{ij}}$- values for the scenario in which both the initial conditions and the sampling times are optimized, and where the ℓ_1, ℓ_2 and ℓ_∞ distance functions are used.

compromise experiment can also be used to judge the experiments obtained.

4. Conclusions

In this paper, a method was presented to design an experiment to simultaneously improve the accuracy of the parameter estimates of several rival models. Since the optimal experiment for one model may not be optimal for another one, the designed experiment is called a compromise experiment. The latter is defined as an experiment that is not optimal for any of the individual models, but sufficiently informative to improve the overall accuracy of the parameters of all rival models.

The problem of designing such a compromise experiment is approached as a multi-objective problem, and the proposed ideal

point method can be applied to experimental design problems with experimental degrees of freedom of all types (manipulations, initial conditions and sampling times). Because closeness can be defined in several ways, the ℓ_1, ℓ_2 and ℓ_∞ distance functions were considered.

The ideal point method was illustrated by applying it in a case study where nine rival models are proposed to describe the kinetics of an enzyme-catalyzed reaction (glucokinase). This was done for a scenario in which only the sampling times were optimized, one in which the initial conditions were optimized, and one in which both the initial conditions and the sampling times were optimized. The results showed that when more experimental degrees of freedom are available, the optimal experiments for the individual models become more and more specific, which makes the design of a compromise rather challenging. Nevertheless, the ideal point method proved to be capable of designing compromise experiments in each of the scenarios, and the results for this case study suggested that the use of the ℓ_2 distance function is preferred over the use of the ℓ_1 and ℓ_∞ distance functions.

Acknowledgments

The authors want to thank the Institute for the Promotion of Innovation by Science and Technology in Flanders for financial support in the framework of SBO-Project 040125 (MEMORE). Peter Vanrolleghem holds the Canada Research Chair on Water Quality Modelling.

References

Asprey, S.P., Macchietto, S., 2000. Statistical tools for optimal dynamic model building. Computers and Chemical Engineering 24, 1261–1267.

Atkinson, A.C., Donev, A.N., 1992. Optimum Experimental Design. Oxford University Press, New York, pp. 328.

Baltes, M., Schneider, R., Sturm, C., Reuss, M., 1994. Optimal experimental design for parameter estimation in unstructured growth models. Biotechnology Progress 10, 480–488.

Burke, A.L., Duever, T.A., Penlidis, A., 1996. An experimental verification of statistical discrimination between the terminal and penultimate polymerization models. Journal of Polymer Science: Part A: Polymer Chemistry 34, 2665–2678.

Burke, A.L., Duever, T.A., Penlidis, A., 1997. Discriminating between the terminal and penultimate models using designed experiments: an overview. Industrial and Engineering Chemistry Research 36, 1016–1035.

Buzzi-Ferraris, G., Forzatti, P., Emig, G., Hofmann, H., 1984. Sequential experimental design procedure for model discrimination in the case of multiple responses. Chemical Engineering Science 39 (1), 81–85.

Cardoso, M.F., Salcedo, R.L., Feyo de Azevedo, S., 1996. The simplex-simulated annealing approach to continuous non-linear optimization. Computers and Chemical Engineering 20 (9), 1065–1080.

Chen, B.H., Asprey, S.P., 2003. On the design of optimally informative dynamic experiments for model discrimination in multiresponse nonlinear situations. Industrial and Engineering Chemistry Research 42, 1379–1390.

Deb, K., 2001. Multi-Objective Optimization using Evolutionary Algorithms. Wiley, New York 515pp.

Dette, H., Kwiecien, R., 2004. A comparison of sequential and non-sequential designs for discrimination between nested regression models. Biometrika 91 (1), 165–176.

Dochain, D., Vanrolleghem, P.A., 2001. Dynamical Modelling and Estimation in Wastewater Treatment Processes. IWA Publishing 360pp.

Donckels, B.M.R., De Pauw, D.J.W., De Baets, B., Maertens, J., Vanrolleghem, P.A., 2009a. An anticipatory approach to optimal experimental design for model discrimination. Chemometrics and Intelligent Laboratory Systems 95 (1), 53–63.

Donckels, B.M.R., De Pauw, D.J.W., Vanrolleghem, P.A., De Baets, B., 2009b. A kernel-based method to determine optimal sampling times for the simultaneous estimation of the parameters of rival mathematical models. Journal of Computational Chemistry 30 (13), 2064–2077.

Goel, T., Vaidyanathan, R., Haftka, R.T., Shyy, W., Queipo, N.V., Tucker, K., 2007. Response surface approximation of Pareto optimal front in multi-objective optimization. Computer Methods in Applied Mechanics and Engineering 196, 879–893.

Goodwin, G.C., Payne, R.L., 1977. Dynamic System Identification: Experiment Design and Data Analysis. Academic Press, New York 299pp.

Hoffmann, A., Levchenko, A., Scott, M., Baltimore, D., 2002. The NF-kB/IkB signaling module: temporal control and selective gene activation. Science 298, 1241–1245.

Hill, W.J., Hunter, W.G., Wichern, D.W., 1968. A joint design criterion for the dual problem of model discrimination and parameter estimation. Technometrics 10 (1), 145–160.

Hunter, W.G., Reiner, A.M., 1965. Designs for discriminating between two rival models. Technometrics 7, 307–323.

Jiang, T., Kennedy, M.D., Guinzbourg, B.F., Vanrolleghem, P.A., Schippers, J.C., 2005. Optimising the operation of a MBR pilot plant by quantitative analysis of the membrane fouling mechanism. Water Science and Technology 51 (6–7), 19–25.

Kitano, H., 2002. Computational systems biology. Science 420, 206–210.

Kirkpatrick, S., Gelatt, C.D., Vecchi, M.P., 1983. Optimization by simulated annealing. Science 220, 671–680.

Kremling, A., Fischer, S., Gadkar, K., Doyle, F.J., Sauter, T., Bullinger, E., Allgöwer, F., Gilles, E.D., 2004. A benchmark for methods in reverse engineering and model discrimination: problem formulation and solutions. Genome Research 14, 1773–1785.

Läuter, E., 1974. Experimental design for a class of models. Statistics: A Journal of Theoretical and Applied Statistics 5 (4), 379–398.

Lee, J., Lee, S.Y., Park, S., Middelberg, A.P.J., 1999. Control of fed-batch fermentations. Biotechnology Advances 17, 29–48.

Ljung, L., 1999. System Identification, Theory for the User. Prentice-Hall, Englewood Cliffs, NJ 608pp.

Marler, R.T., Arora, J.S., 2004. Survey of multi-objective optimization methods for engineering. Structural and Multidisciplinary Optimization 26, 369–395.

Marsili-Libelli, S., Guerrizio, S., Checchi, N., 2003. Confidence regions of estimated parameters for ecological systems. Ecological Modelling 165, 127–146.

Mehra, R., 1974. Optimal input signals for parameter estimation in dynamic systems–Survey and new results. IEEE Transactions on Automatic Control 19 (6), 753–768.

Monasterio, O., Cárdenas, M.L., 2003. Kinetic studies of rat liver hexokinase D ('glucokinase') in non-co-operative conditions showing an ordered mechanism with MgADP as the last product to be released. Biochemical Journal 371, 29–38.

Munack, A., 1991. Optimization of sampling. In: Schügerl, K. (Ed.), Biotechnology, a Multi-volume Comprehensive Treatise, Measuring, Modelling and Control, vol. 4. VCH, Weinheim, pp. 251–264.

Nelder, J.A., Mead, R., 1965. A simplex method for function minimization. Computer Journal 7, 308–313.

Ogawa, T., Mori, H., Tomita, M., Yoshino, M., 2007. Inhibitory effect of phosphoenolpyruvate on glycolytic enzymes in *Escherichia coli*. Research in Microbiology 158, 159–163.

Omlin, M., Reichert, P., 1999. A comparison of techniques for the estimation of model prediction uncertainty. Ecological Modelling 115 (1), 45–49.

Petersen, B., 2000. Calibration, identifiability and optimal experimental design of activated sludge models. Ph.D. Thesis, Ghent University, 337pp.

Schwaab, M., Silva, F.M., Queipo, C.A., Barreto Jr., A.G., Nele, M., Pinto, J.C., 2006. A new approach for sequential experimental design for model discrimination. Chemical Engineering Science 61, 5791–5806.

Seber, G.A.F., Wild, C.J., 1989. Nonlinear Regression. Wiley, 768pp.

Segel, I.H., 1975. Enzyme Kinetics-Behaviour and Analysis of Rapid Equilibrium and Steady-State Enzyme Systems. Wiley, New York 957pp.

Shirt, R.W., Harris, T.J., Bacon, D.W., 1994. Experimental design considerations for dynamic systems. Industrial and Engineering Chemistry Research 33, 2656–2667.

Ternbach, M.A.B., Bollman, C., Wandrey, C., Takors, R., 2005. Application of model discriminating experimental design for modeling and development of a fermentative fed-batch L-valine production process. Biotechnology and Bioengineering 91 (3), 356–368.

Vanrolleghem, P., Van Daele, M., 1994. Optimal experimental design for structure characterization of biodegradation models: on-line implementation in a respirographic biosensor. Water Science and Technology 30 (4), 243–253.

Vanrolleghem, P.A., Dochain, D., 1998. Bioprocess model identification. In: Van Impe, J.F.M., Vanrolleghem, P.A., Iserentant, D.M. (Eds.), Advanced Instrumentation, Data Interpretation, and Control of Biotechnological Processes. Kluwer Academic Publishers, Dordrecht, pp. 251–318.

Walter, E., Pronzato, L., 1997. Identification of Parameteric Models from Experimental Data. Springer, Berlin, Heidelberg, New York 413pp.